Annual Report 2019/2020

Student: Vladislav Khaustov
Supervisor: Camilla Coletti

National Enterprise for nanoScience and nanoTechnology

Introduction

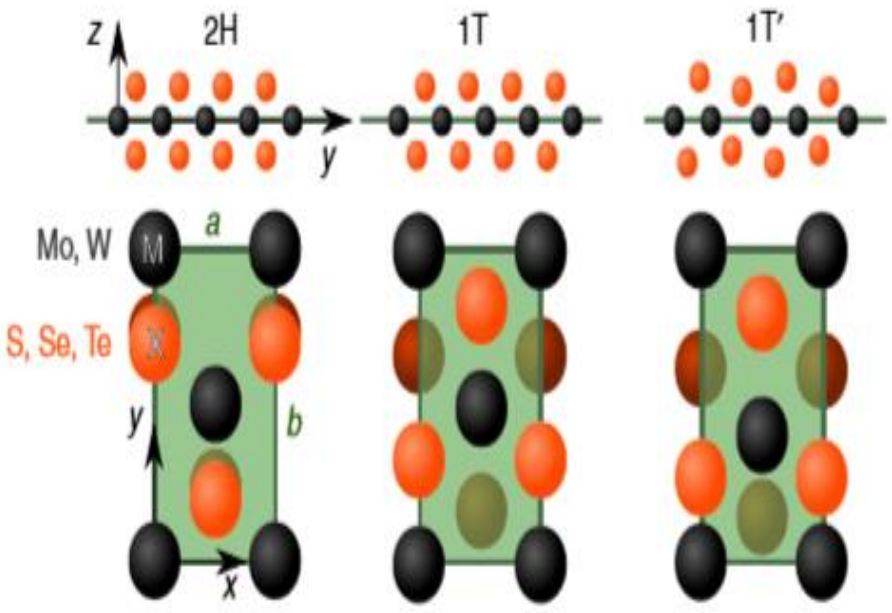

The three crystalline phases of 2D group VI TMDs [1]

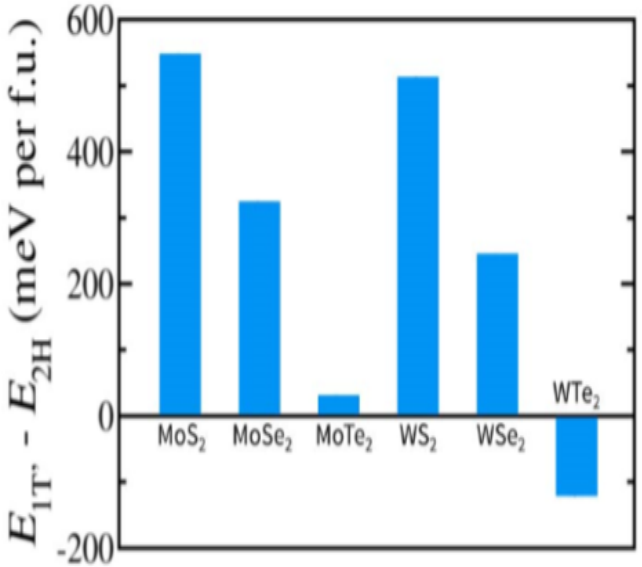

Semilocal DFT-calculated energy differences per formula unit between freely suspended charge-neutral 2H and 1T’ phases of monolayer Mo- and W-dichalcogenides, with spin orbit coupling effects included [2]

Methods	
Straining	
Laser irradiation	
Temperature	
Vacancies	X
Doping/Substitution	
Electrostatic	X
Charge transfer	X

Theory

Gibbs free energy differential

$$dG = -SdT + VdP + \mu_{Te}dN_{Te} + \mu_c dN_c$$

dP=0 $\quad dG_{1T'} = dG_{2H}$

Pairs of Clausius-Clayperon equations

$$\Delta\mu_{Te}dN_{Te} = \Delta SdT$$

$$\Delta\mu_c dN_c = \Delta SdT$$

$$\Delta\mu_{Te}dN_{Te} = -\Delta\mu_c dN_c$$

Where $\Delta\mu_{Te} = \mu_{Te}^{1T'} - \mu_{Te}^{2H}$, $\Delta S = S^{1T'} - S^{2H}$, $\Delta\mu_c = \mu_c^{1T'} - \mu_c^{2H}$

Total entropy difference

$$\Delta S = \Delta S_{phonon} + \Delta S_{electron} + \Delta S_{configuration}$$

$S_{configuration}$ becomes relevant when 2H prefers clusterization and 1T' isolated ordering. [6]

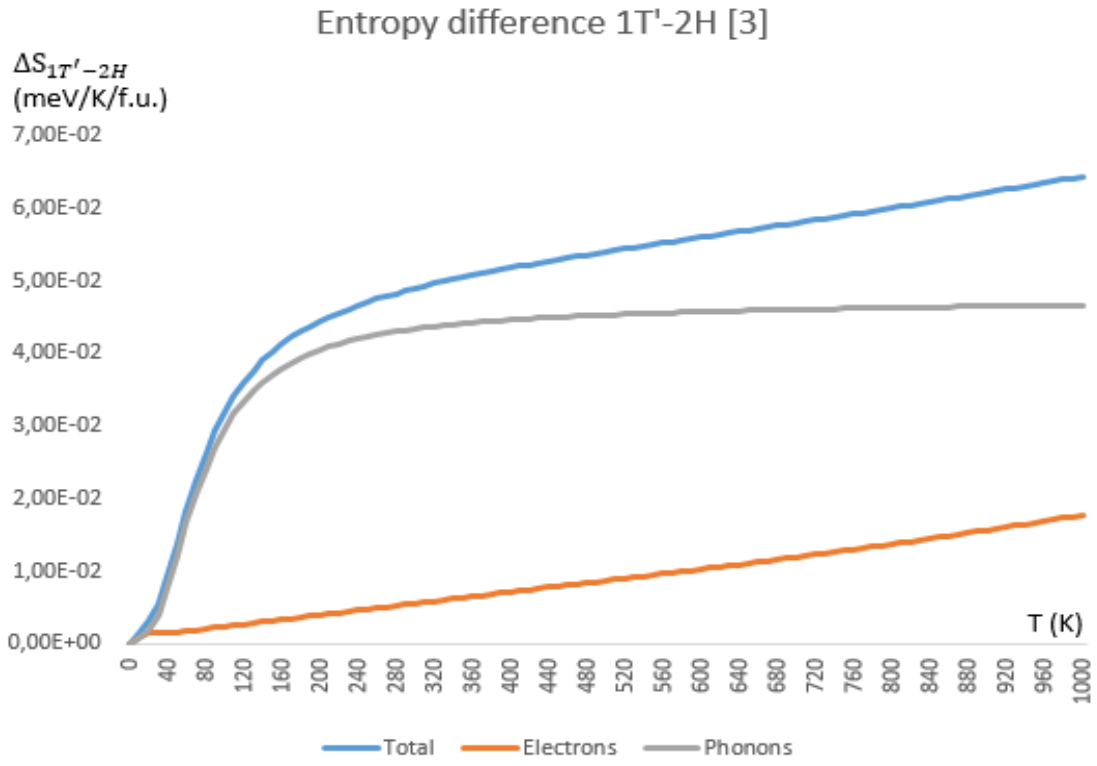

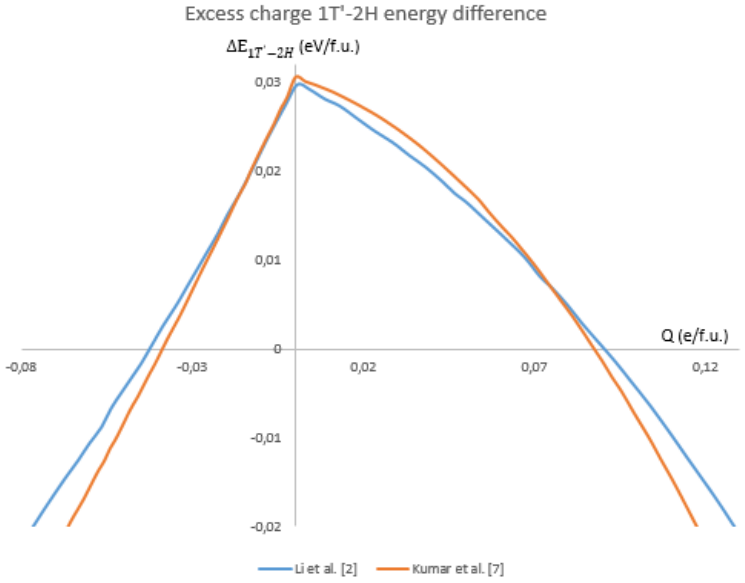

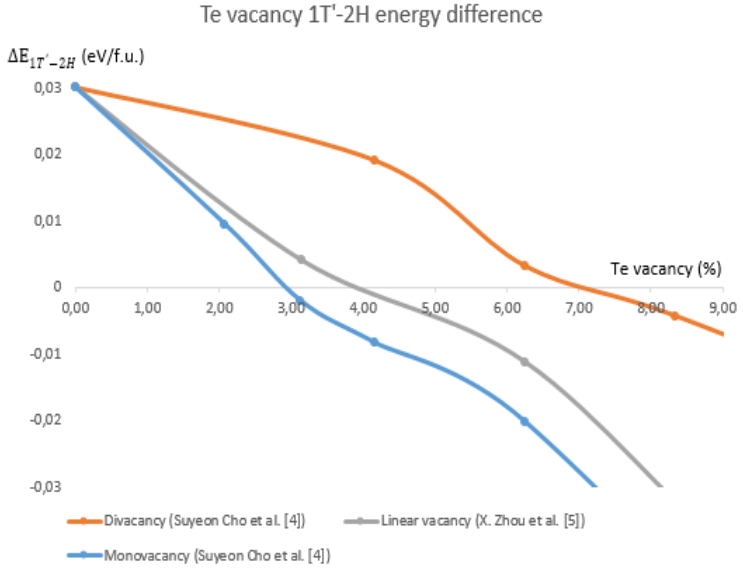

Phase diagrams

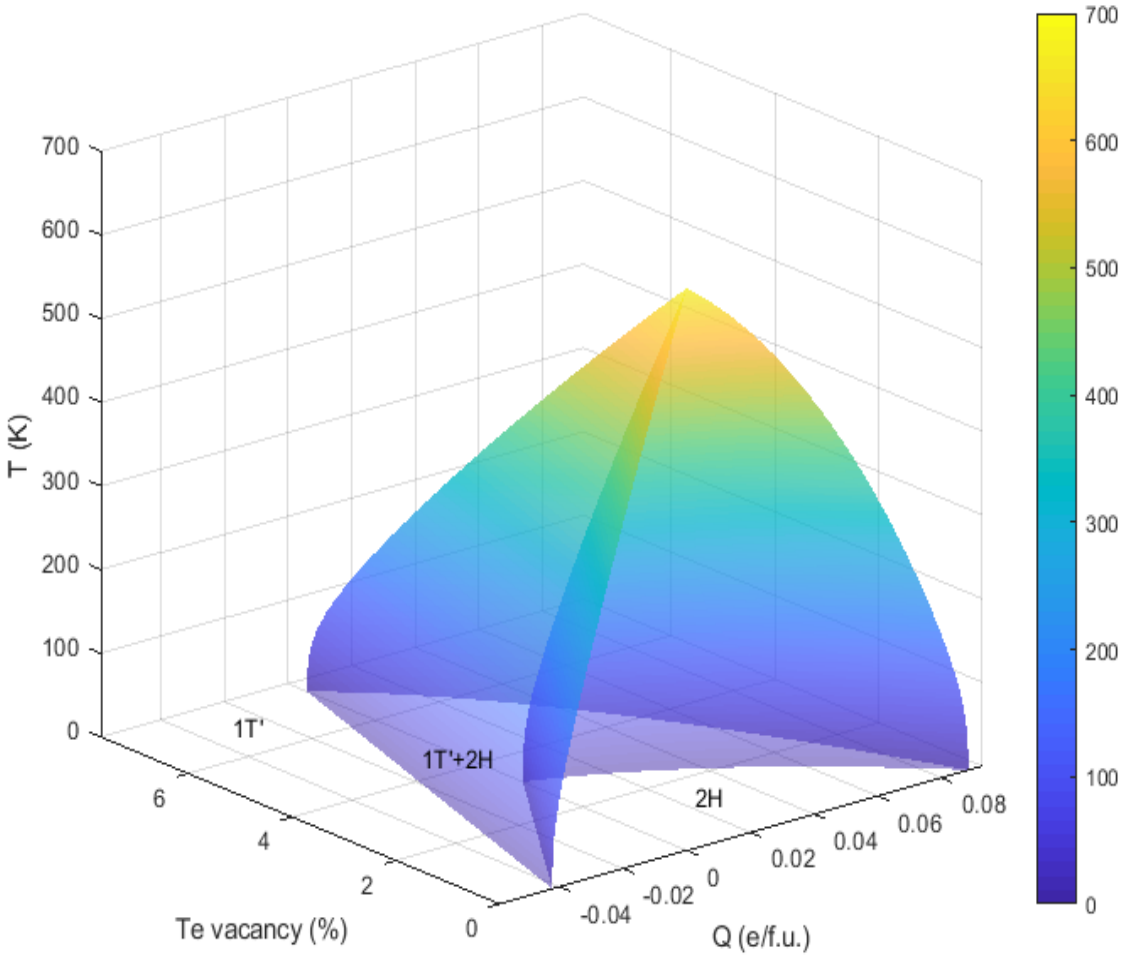

$$\Delta E^{0}_{1T'-2H} = 30\,\frac{\mathrm{meV}}{f.u.}$$

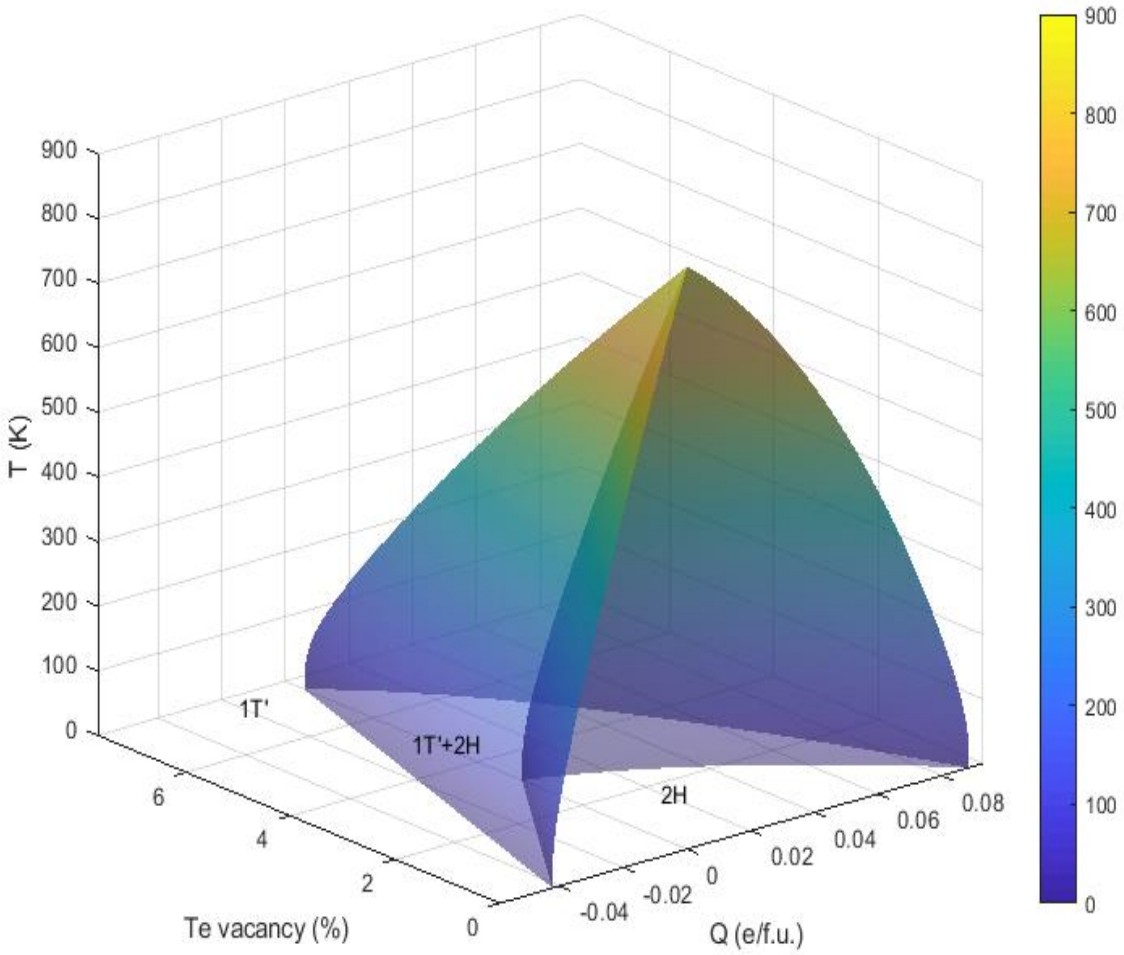

$$\Delta E^{0}_{1T'-2H} = 44\,\frac{\mathrm{meV}}{f.u.}$$

Phase diagrams

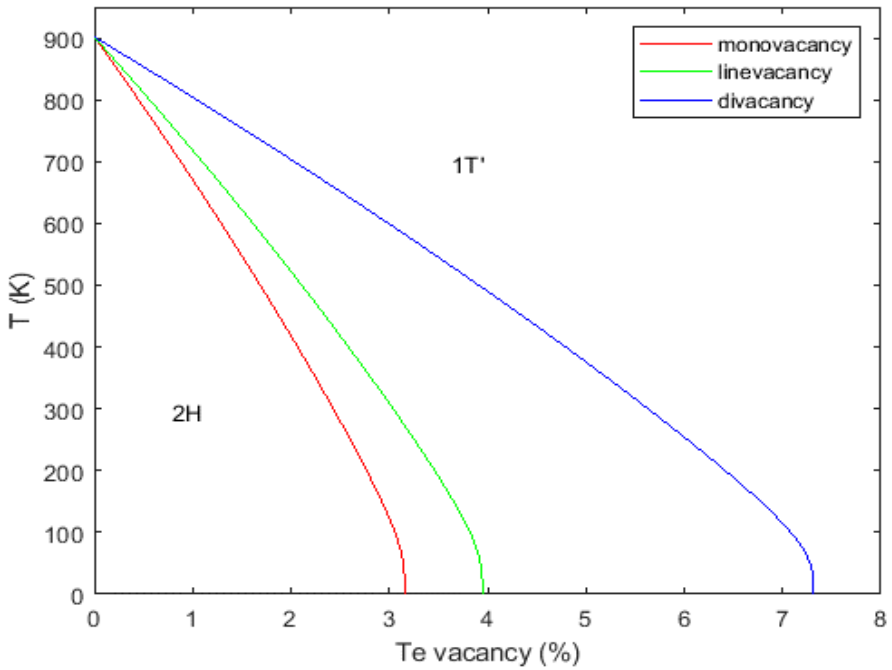

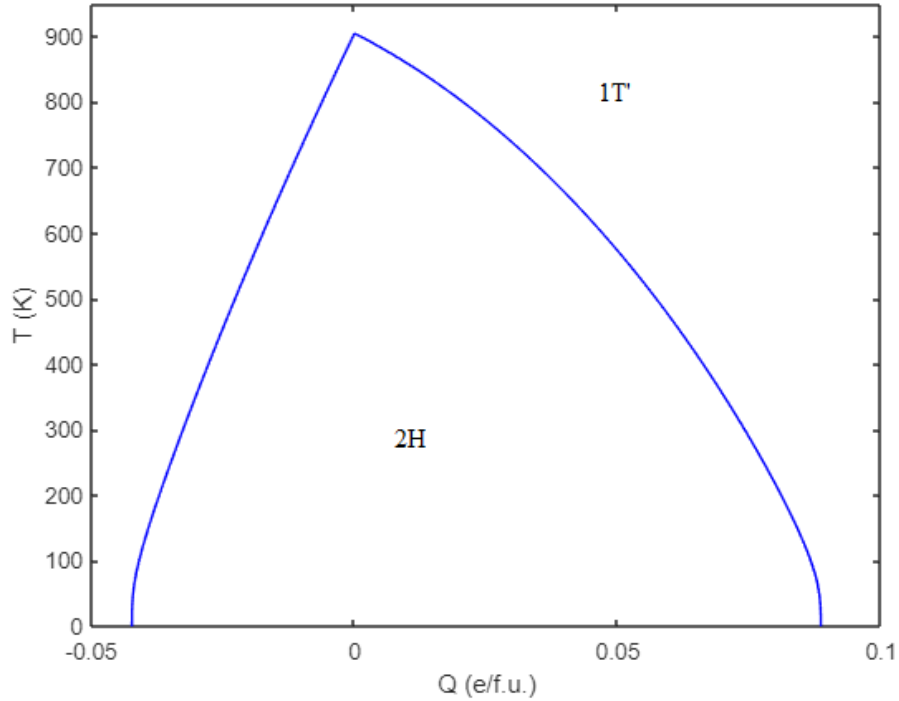

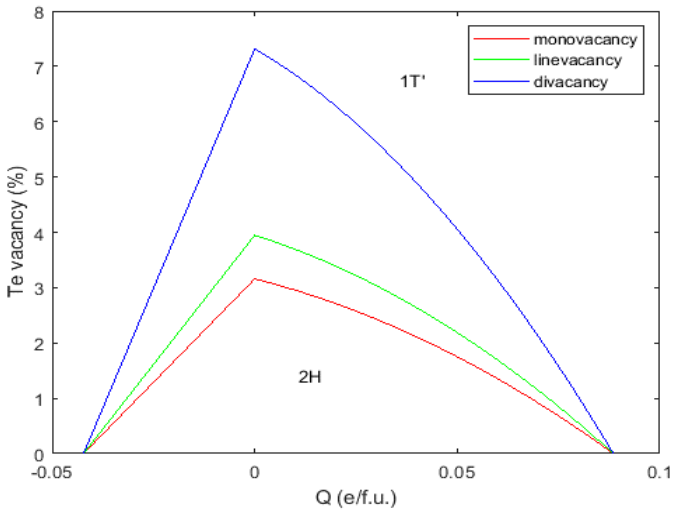

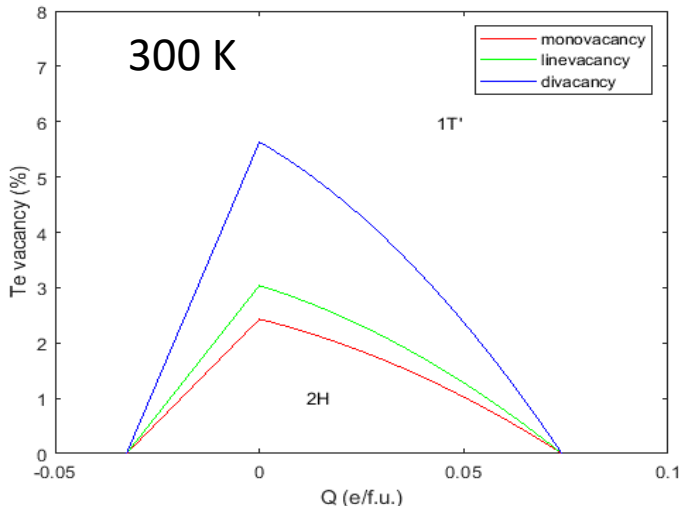

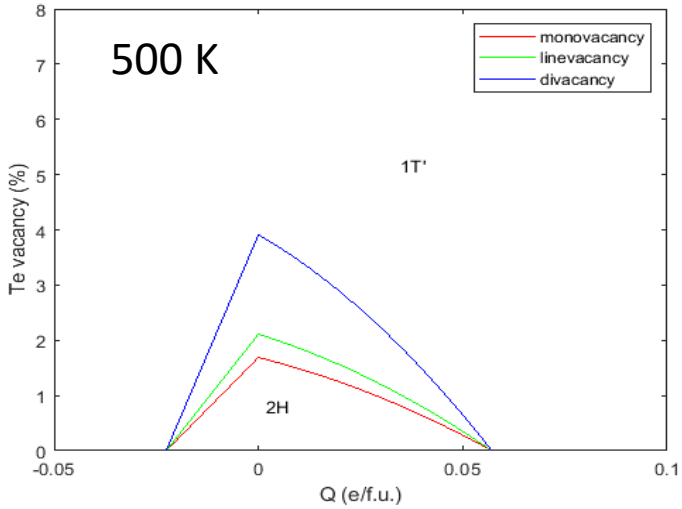

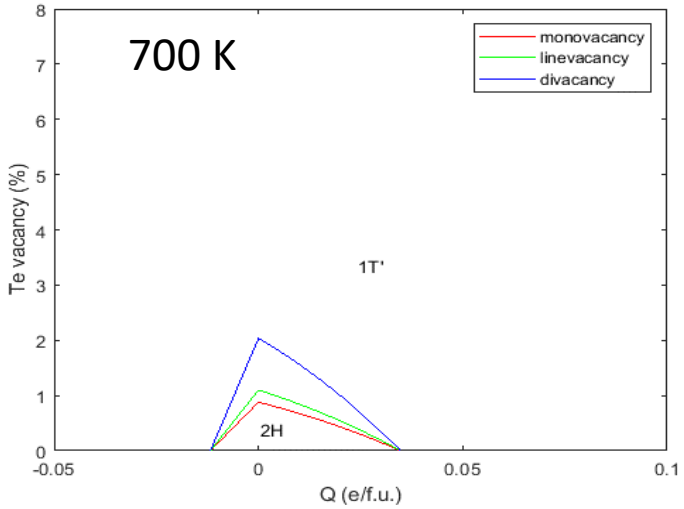

$$\Delta E^{0}_{1T'-2H} = 44\,\frac{\mathrm{meV}}{f.u.}$$

Material growth

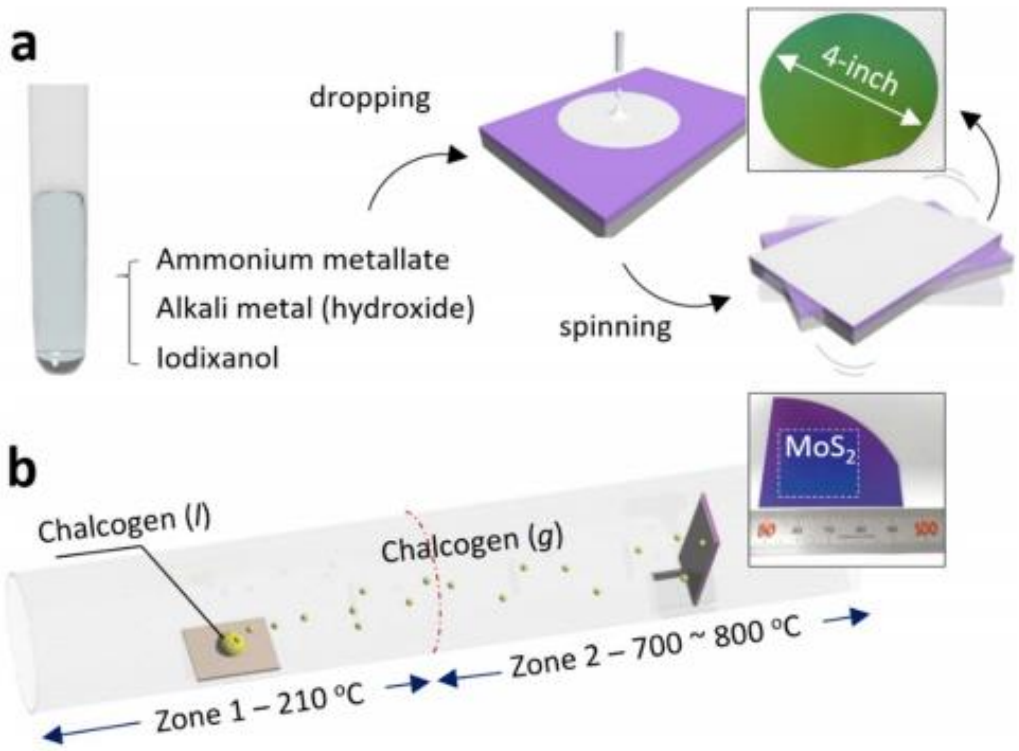

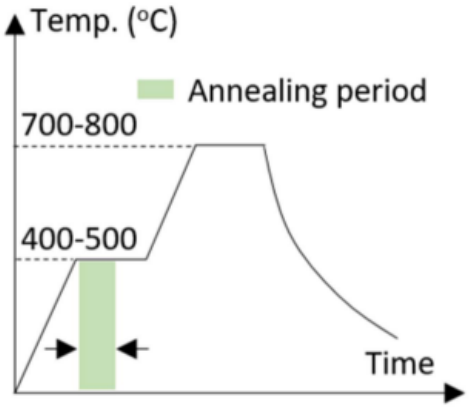

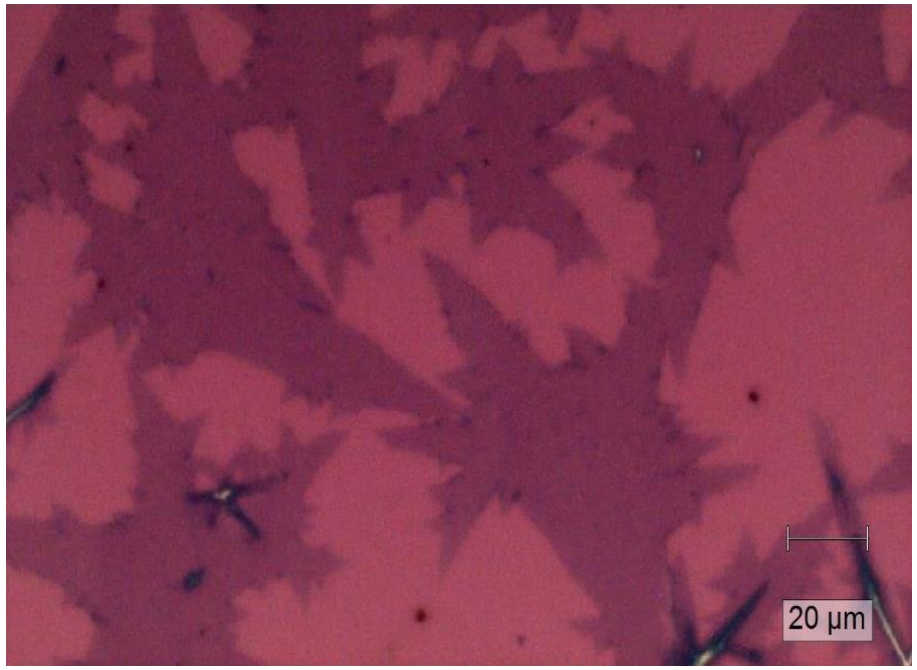

Growth procedure. (a) The solution containing the alkali metal (promoter), ammonium metallate (water-soluble transition metal precursor), and iodixanol dropped and spin-casted onto the clean SiO2 (300 nm)/Si wafer to form the precursor/promoter (P/P) layer. (b) Two-zone CVD chamber with different temperatures. The substrate was loaded in the high temperature region (zone 2) and the solid chalcogen was sublimated in the low temperature region (zone 1). [8]

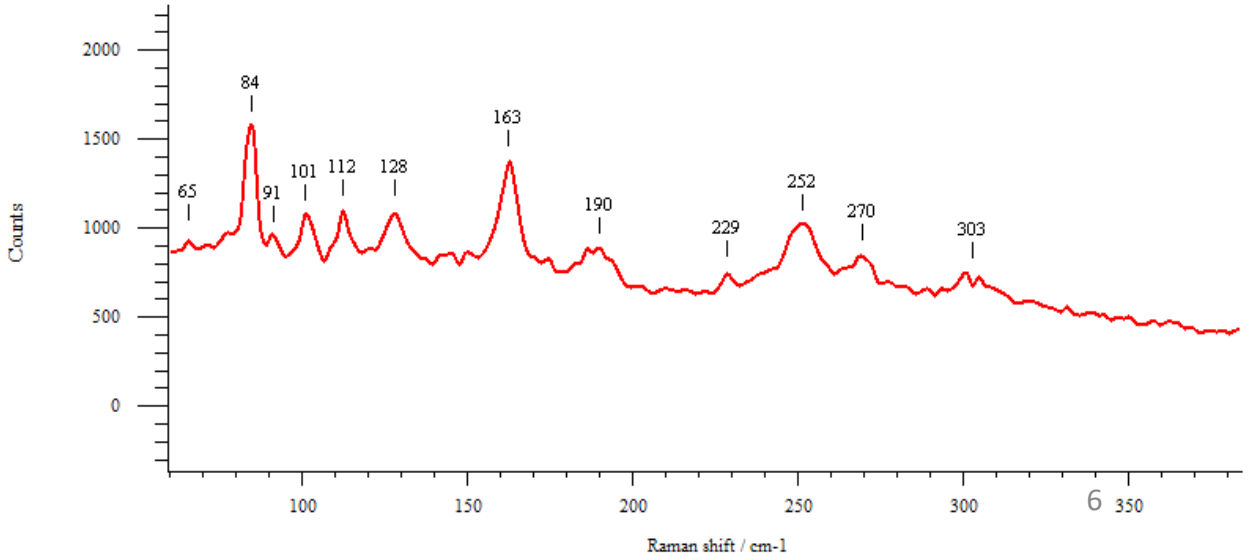

1T’ Raman data

1T’ Raman peak positions	Bg (A’’)	Ag (A’)	Bg (A’’)	Bg (A’’)	Ag (A’)	Ag (A’)	Ag (A’)	Bg (A’’)	Ag (A’)	Ag (A’)	?
Theoretical											
Beams, et al. [9]		78	94	107	111	128	163	192	249	260	
Kan, Min et al. [10]	73.75	80.41		101.01	111.27	125.69	161.1	162.52	254.58	269.22	
Experimental (few-layer to bulk)											
HQ Graphene 1T’ (experimental, bulk)		77.5	94.7	107.2		128.5	163.8			260	
Park et al. (CVD, ~20 nm) [11]				107		126.9	163			256.1	
Zhou et al. (CVD, ?) [12]		78	93		110	128	162			258	
SiO2/MoTe2/hBN (CVD, few layer)		**78**	**93**	**106**	**110**	**128**	**163**	**191**	**254**	**267**	
Experimental (monolayer)											
Empante et al. (CVD, 1L) [13]	*80*	*85*		*102*	*112*	*126*	*162*				
Naylor et al. (CVD, 1L) [14]					*112*	*127*	*161*	*188*	*252*	*269*	
Chen et al. (CVD, 1L) [15]		85	92	102	113	128	164	190	253	270	
Au/MoTe2/hBN (CVD, 1L)		**84**		**101**	**112**	**127**	**162**	**188**	**250**	**271**	**302**
Pt/MoTe2/hBN (CVD, 1L)	**69**	**85**		**101**	**113**	**128**	**162**	**189**	**251**	**270**	
SiO2/MoTe2/hBN (CVD, 1L)		**85**		**101**	**113**	**128**	**162**	**189**	**251**	**271**	**302**

2H Raman data

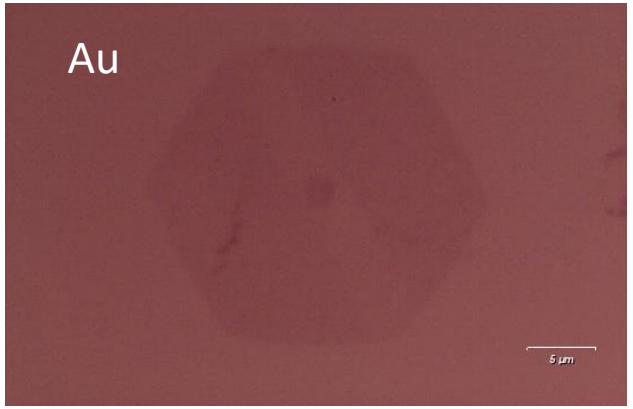

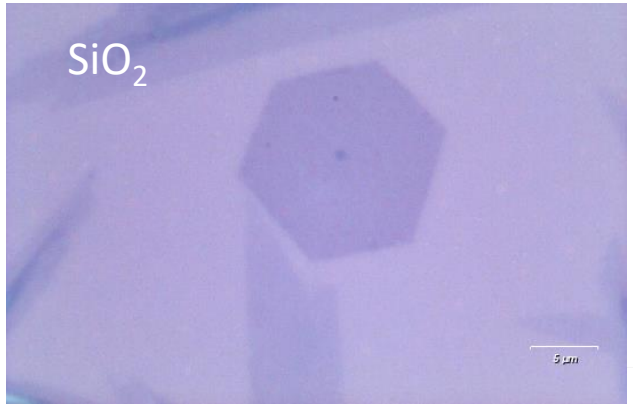

2H Raman peak positions	E’	-	A_1’	-	E’’	A_2’	-	I(A_2’/E’’)
Kan, Min et al. (calculated) (10)	114.54		170.03		230.16			
Yamamoto et al. (calculated, 1L to bulk)(16)	120.2		178.1		242.3	300.5		
Yamamoto et al. (experiment, 1L)(16)		138	172	185	236.5	291		0
Au/MoTe2/hBN (CVD, 1L)	**116**	**136**	**171**	**183**	**234**	**291**		**0-0.2**
Pt/MoTe2/hBN (CVD, 1L)	**102**	**137**	**170**	**183**	**235**	**290**	**302**	**0-0.1**
SiO2/MoTe2/hBN (CVD, 1L)	**104**	**137**	**168**	**183**	**234**		**302**	**0**

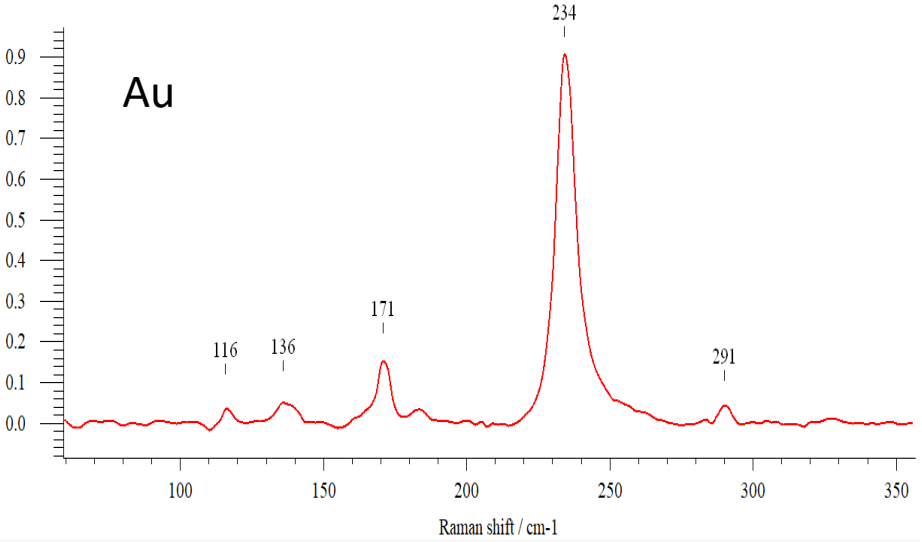

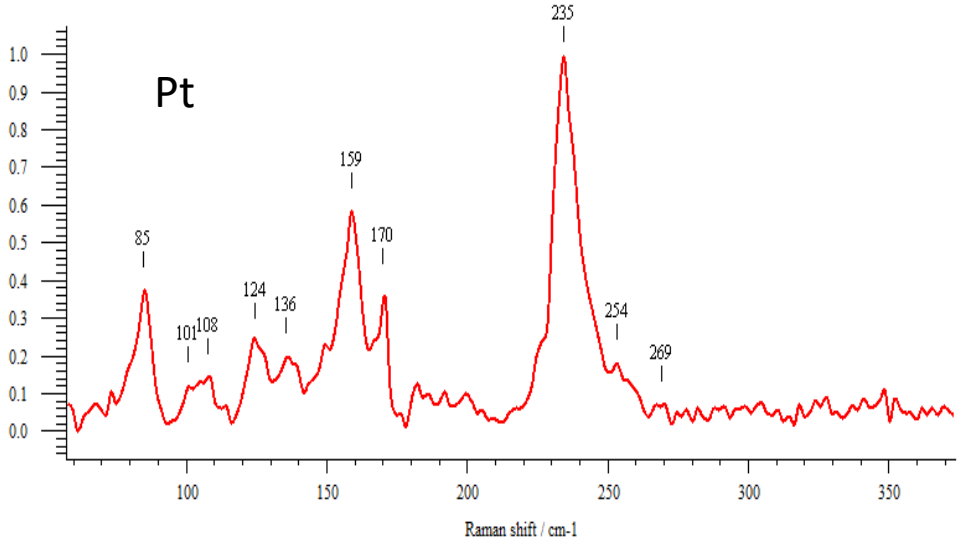

CAFM and STM experiments

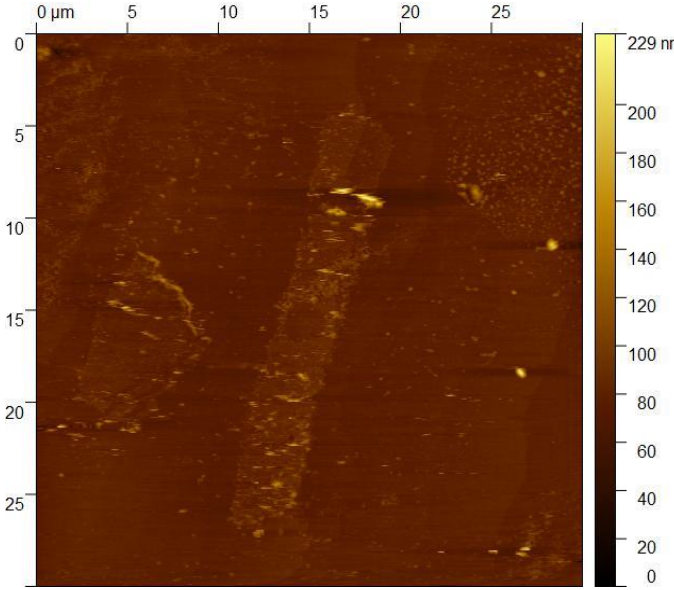

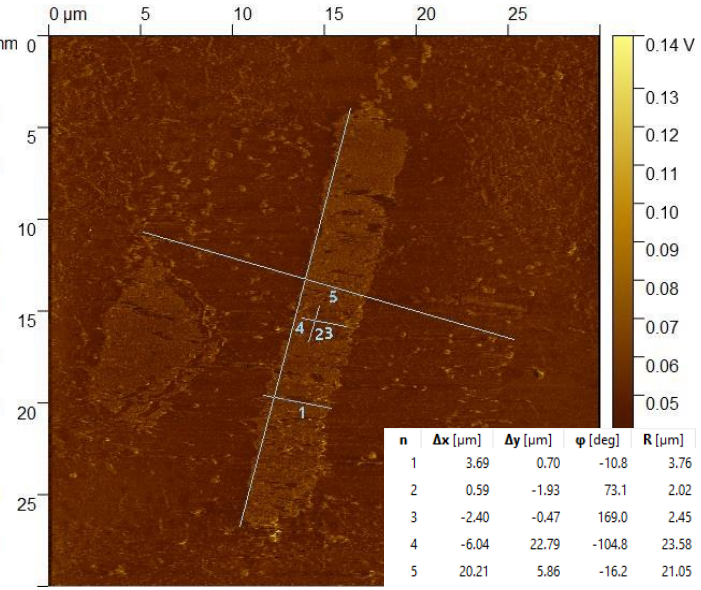

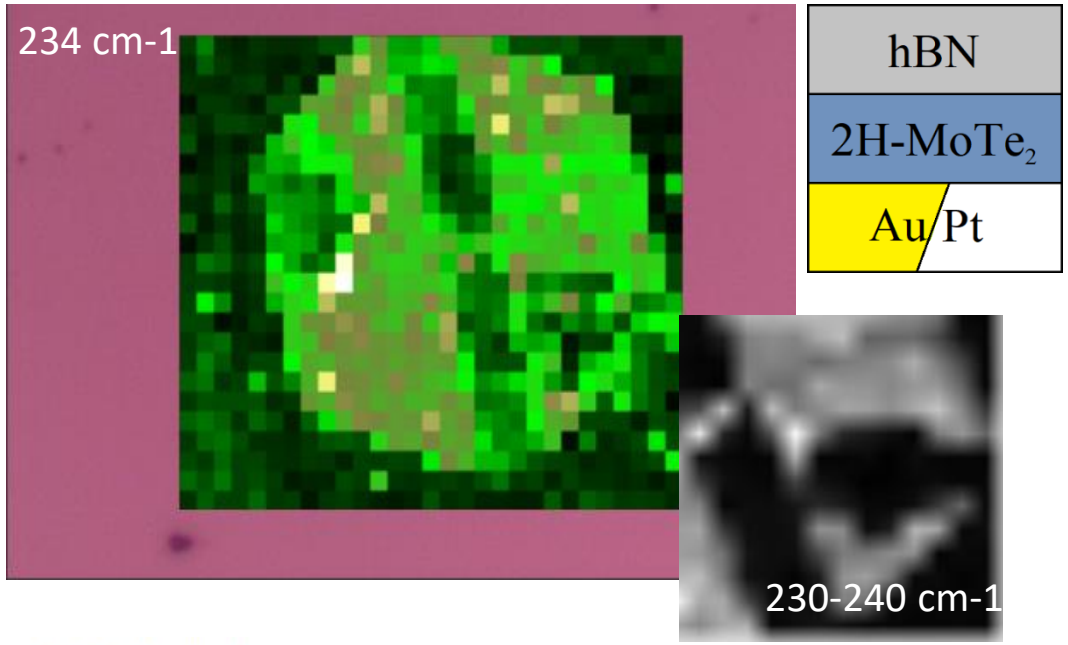

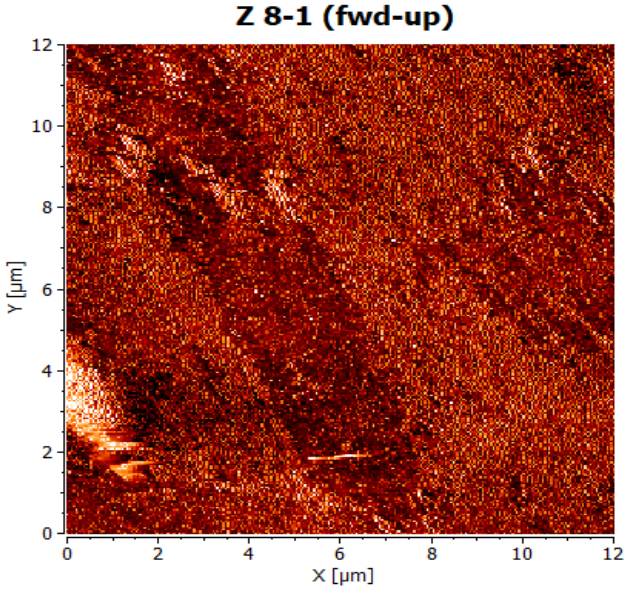

I = 180 pA
V = 2 V

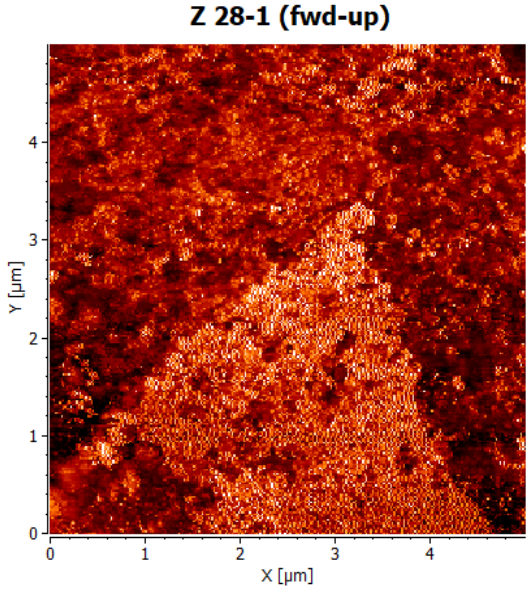

Before 4.5 V

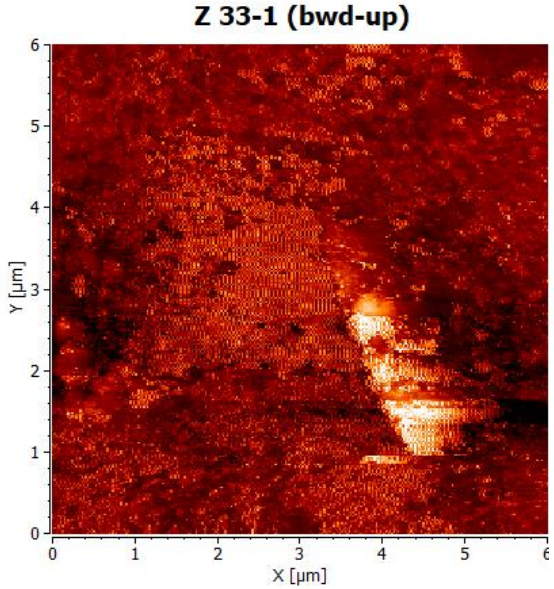

After 4.5 V

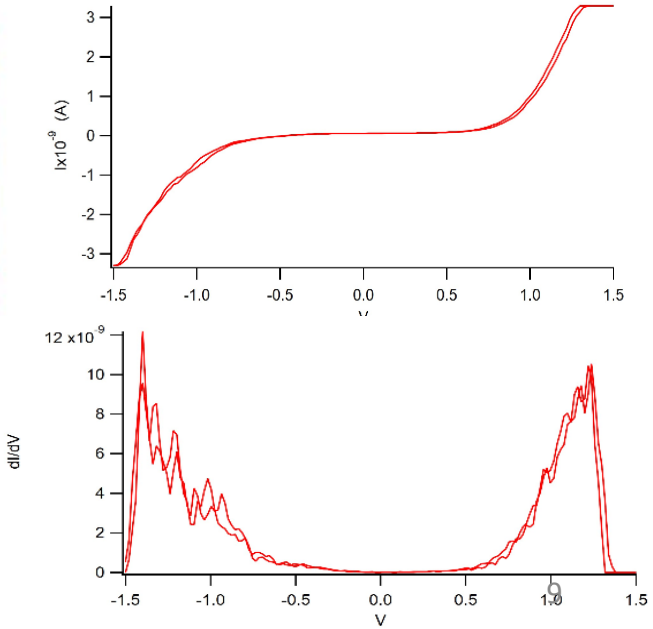

2H-1T’ Phase transition

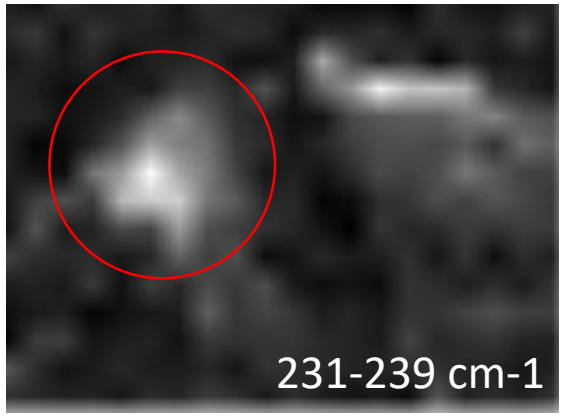

1T’ Raman peak positions after 2H > 1T’ phase change	Bg (A’’) 70	Ag (A’) 85	Bg (A’’) 93	Bg (A’’) 102	Ag (A’) 113	Ag (A’) 128	Ag (A’) 163	Bg (A’’) 189	Ag (A’) 251	Ag (A’) 270
Song et al. (strain phase change, >20 nm) [17]					120	140				
Cho et al. (laser phase change, bulk) [18]					123	138				
Tan et al. (laser phase change, bulk) [19]					125	140				
Wang et al. (electrostatic, 1L) [20]							*167.5*			
Zakhidov et al. (electrostatic, electrochemical, 1L to bulk) [21]	*78*	*90*			*120*	*140*	*168*			
Shi et al. (THZ, 1L) [22]							163.3			
Kim et al. (2D electride, bulk) [23]					125	140	166	191		270

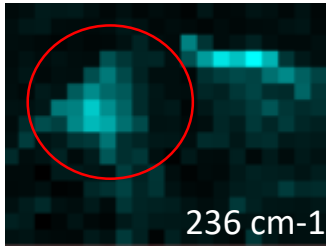

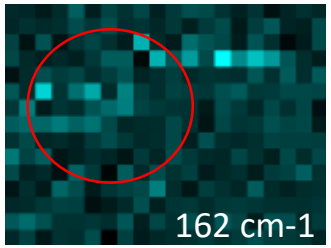

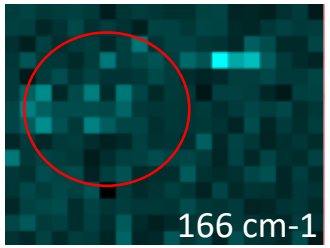

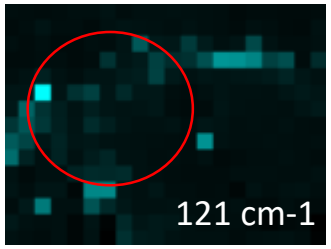

Material	Peak, cm -1
2H-$MoTe_2$	235, 170
1T’-$MoTe_2$	85, 162
Te metal [24]	120, 140

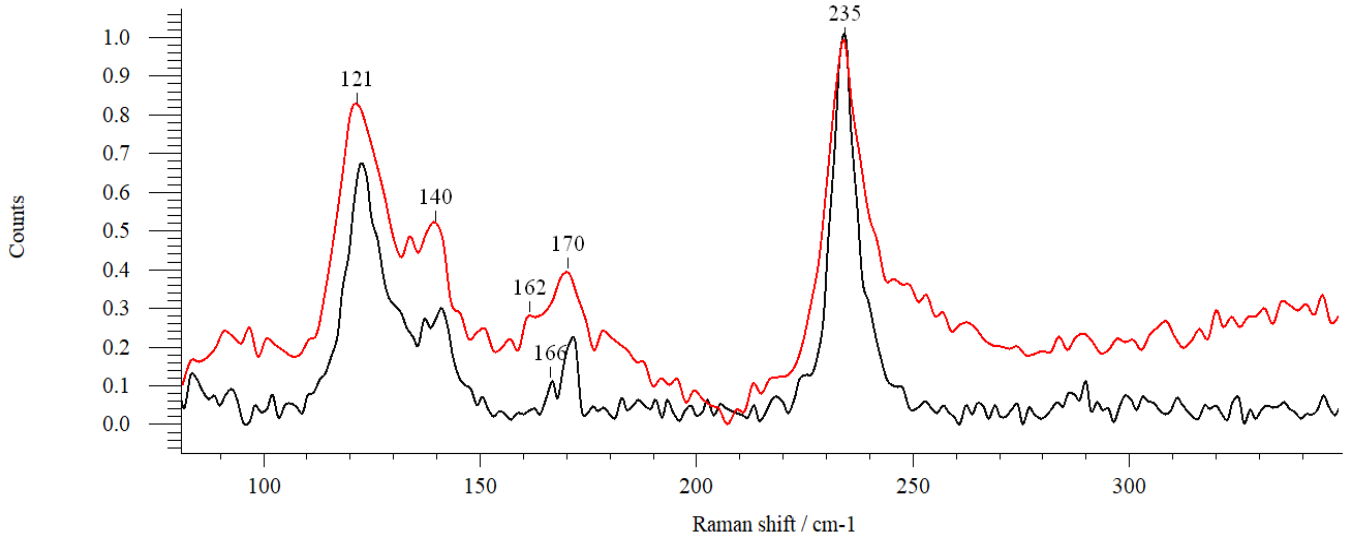

1) Duerloo, Karel-Alexander N., Yao Li, and Evan J. Reed. "Structural phase transitions in two-dimensional Mo-and W-dichalcogenide monolayers." *Nature communications* 5 (2014): 4214.

2) Yao Li, Karel-Alexander N Duerloo, Kerry Wauson, and Evan J Reed. Structural semiconductor to-semimetal phase transition in two-dimensional materials induced by electrostatic gating. Nature communications, 7:10671, 2016.

3) Rehn, Daniel A., et al. "Theoretical potential for low energy consumption phase change memory utilizing electrostatically-induced structural phase transitions in 2D materials." *npj Computational Materials* 4.1 (2018): 1-9.

4) Cho, Suyeon, et al. "Phase patterning for ohmic homojunction contact in MoTe2." *Science* 349.6248 (2015): 625-628.

5) Zhou, Xiangyu, et al. "Electron-injection driven phase transition in two-dimensional transition metal dichalcogenides." *Journal of Materials Chemistry C* 8.13 (2020): 4432-4440.

6) Tang, Qing. "Tuning the phase stability of Mo-based TMD monolayers through coupled vacancy defects and lattice strain." *Journal of Materials Chemistry C* 6.35 (2018): 9561-9568.

7) Kumar, Abhinav, Alejandro Strachan, and Nicolas Onofrio. "Prediction of low energy phase transition in metal doped MoTe 2 from first principle calculations." *Journal of Applied Physics* 125.20 (2019): 204303.

8) Kim, Hyun, et al. "Role of alkali metal promoter in enhancing lateral growth of monolayer transition metal dichalcogenides." *Nanotechnology* 28.36 (2017): 36LT01.

9) Beams, R.; Cançado, L. G.; Krylyuk, S.; Kalish, I.; Kalanyan, B.; Singh, A. K.; Choudhary, K.; Bruma, A.; Vora, P. M.; Tavazza, F.; Davydov, A. V.; Stranick, S. J. Characterization of Few-Layer 1T' MoTe2 by Polarization-Resolved Second Harmonic Generation and Raman Scattering. ACS Nano 2016, 10, 9626–9636.

10) Kan, Min, et al. "Phase stability and Raman vibration of the molybdenum ditelluride (MoTe 2) monolayer." Physical Chemistry Chemical Physics 17.22 (2015): 1486614871.

11)) Park, J. C.; Yun, S. J.; Kim, H.; Park, J.-H.; Chae, S. H.; An, S.-J.; Kim, J.-G.; Kim, S. M.; Kim, K. K.; Lee, Y. H. Phase-Engineered Synthesis of Centimeter-Scale 1T'- and 2H-Molybdenum Ditelluride Thin Films. ACS Nano 2015, 9, 6548–6554.

12) Zhou, L.; Zubair, A.; Wang, Z.; Zhang, X.; Ouyang, F.; Xu, K.; Fang, W.; Ueno, K.; Li, J.; Palacios, T.; Kong, J.; Dresselhaus, M. S. Synthesis of High-Quality Large-Area Homogenous 1T' MoTe2 from Chemical Vapor Deposition. Adv. Mater. 2016, 9526–9531.

13) Empante, T. A.; Zhou, Y.; Klee, V.; Nguyen, A. E.; Lu, I.-H.; Valentin, M. D.; Naghibi Alvillar, S. A.; Preciado, E.; Berges, A. J.; Merida, C. S.; Gomez, M.; Bobek, S.; Isarraraz, M.; Reed, E. J.; Bartels, L. Chemical Vapor Deposition Growth of Few-Layer MoTe2 in the 2H, 1T', and 1T Phases: Tunable Properties of MoTe2 Films. ACS Nano 2017, 11, 900–905.

14) Naylor, C. H.; Parkin, W. M.; Ping, J.; Gao, Z.; Zhou, Y. R.; Kim, Y.; Streller, F.; Carpick, R. W.; Rappe, A. M.; Drndić, M.; Kikkawa, J. M.; Johnson, A. T. C. Monolayer Single-Crystal 1T'-MoTe2 Grown by Chemical Vapor Deposition Exhibits Weak Antilocalization Effect. Nano Lett. 2016, 16, 4297–4304.

15) Chen, S.-Y., Naylor, C. H., Goldstein, T., Johnson, A. T. C. & Yan, J. Intrinsic phonon bands in high-quality monolayer T' Molybdenum Ditelluride. ACS Nano 11, 814-820 (2017).

16) Yamamoto, Mahito, et al. "Strong enhancement of Raman scattering from a bulk-inactive vibrational mode in few-layer MoTe2." *Acs Nano* 8.4 (2014): 3895-3903.

17) Song, S.; Keum, D. H.; Cho, S.; Perello, D.; Kim, Y.; Lee, Y. H. Room Temperature Semiconductor– Metal Transition of MoTe2 Thin Films Engineered by Strain. Nano Lett. 2016, 16, 188–193.

18) Cho, S.; Kim, S.; Kim, J. H.; Zhao, J.; Seok, J.; Keum, D. H.; Baik, J.; Choe, D.-H.; Chang, K. J.; Suenaga, K.; Kim, S. W.; Lee, Y. H.; Yang, H. Phase Patterning for Ohmic Homojunction Contact in MoTe2. Science 2015, 349, 625–628.

19) Tan, Y.; Luo, F.; Zhu, M.; Xu, X.; Ye, Y.; Li, B.; Wang, G.; Luo, W.; Zheng, X.; Wu, N.; Yu, Y.; Qin, S.; Zhang, X.-A. Controllable 2H-to-1T' Phase Transition in Few-Layer MoTe2. Nanoscale 2018, 10, 19964–19971.

20) Wang, Y.; Xiao, J.; Zhu, H.; Li, Y.; Alsaid, Y.; Fong, K. Y.; Zhou, Y.; Wang, S.; Shi, W.; Wang, Y.; Zettl, A.; Reed, E. J.; Zhang, X. Structural Phase Transition in Monolayer MoTe2 Driven by Electrostatic Doping. Nature 2017, 550, 487–491.

21) Zakhidov, Dante, et al. "Reversible Electrochemical Phase Change in Monolayer to Bulk-like MoTe2 by Ionic Liquid Gating." *ACS nano* 14.3 (2020): 2894-2903.

22) Shi, Jiaojian, et al. "Terahertz-driven irreversible topological phase transition in two-dimensional MoTe $ _ {2} $." *arXiv preprint arXiv:1910.13609* (2019).

23) Kim, Sera, et al. "Long-range lattice engineering of MoTe2 by a 2D electride." *Nano letters* 17.6 (2017): 3363-3368.

24) Churchill, Hugh OH, et al. "Toward Single Atom Chains with Exfoliated Tellurium." *Nanoscale Research Letters* 12.1 (2017): 488.

Thank you for your attention